water oxidation cycle,[50a] a recently modified[50b,c] version of which incorporates the Mn_4O_3 core at S_2. We have also proposed that S_3 now possesses the second substrate (H_2O) molecule in a deprotonated form to yield a $[Mn_4O_4]^{6+}$ core at S_3; again, binding of a second hard ligand (as OH^- or O^{2-}) is proposed to lower the potential of the S_2/S_3 couple to within the $PSII^+$ limit. Thus, a synergistic relationship is proposed: the Mn_4O_2 core acts as a template to bind, deprotonate, bring together, and facilitate oxidative coupling of the two H_2O molecules to O_2, and, in return, the bound substrates lower the potential required to access the higher S_n states; this is summarized below. Subsequent oxidation

$$\underset{S_0}{[Mn_4O_2]^{7+}} \xrightarrow{-e} \underset{S_1}{[Mn_4O_2]^{8+}} \xrightarrow[-2H^+]{-e,\ +H_2O} \underset{S_2}{[Mn_4O_3]^{7+}} \xrightarrow[-2H^+]{-e,\ +H_2O} \underset{S_3}{[Mn_4O_4]^{6+}}$$

to S_4 spontaneously evolves O_2 returning the Mn assembly to $[Mn_4O_2]^{7+}$ (S_0). More detail will be provided with our full report of the $[Mn_4O_3]^{7+}$-containing products.

Summary and Conclusions

Treatment of trinuclear complexes containing the Mn_3O core with chelating bipy allows high-yield access into a new class of tetranuclear Mn complexes containing the Mn_4O_2 core. The products can be obtained in three different oxidation levels by appropriate choice of the Mn_3O reagent employed. The Mn_4O_2 complexes possess structural and other features bearing correspondence to the native site of the water oxidation system, suggesting that synthetic models of the latter in its S_{-1}, S_0, and S_1 states may have been obtained. A search for tetranuclear species corresponding to the S_2 and S_3 native levels is in progress, and preliminary work has been communicated.[49] Overall, availability of low molecular weight synthetic representations should prove invaluable in the continuing multidisciplinary investigation of the precise structure and mode of action of this important and complex biological system.

Acknowledgment. This work was supported by NSF Grant CHE-8507748 (to G.C.), by NIH Grant HL13652 (to D.N.H.), and we thank the Bloomington Academic Computing Service for a gift of computer time. C.C. thanks the Chemistry Department at Indiana University for Ira E. Lee and Harry G. Day Undergraduate Research Scholarships. NMR instrumentation at Indiana University was funded by NSF Grant CHE-8105004.

Supplementary Material Available: Complete listings of atomic coordinates, isotropic and anisotropic thermal parameters, bond lengths and angles, magnetic susceptibility and magnetization, and EPR data (24 pages); listings of observed and calculated structure factors for **1** and **4** (15 pages). Ordering information is given on any current masthead page. Complete copies of the MSC structure reports (No. 86162 and No. 86084 for **1** and **4**, respectively) are available on request from the Indiana University Chemistry Library.

(50) (a) Vincent, J. B.; Christou, G. *Inorg. Chim. Acta* **1987**, *L41*, 136. (b) Christou, G.; Vincent, J. B. *Metal Clusters in Proteins*; Que, L., Ed.; ACS Symposium Series 372; American Chemical Society: Washington, DC, 1988; Chapter 12. (c) Christou, G.; Vincent, J. B. *Biochim. Biophys. Acta* **1988**, *895*, 259.

(51) See Supplementary Material.

Insertions of Electrophiles into Metal–Carbon Bonds: Formation of New Carbon–Nitrogen Linkages Mediated by the (η^5-Cyclopentadienyl)dinitrosylchromium Group[1,2]

Peter Legzdins,*[3a] George B. Richter-Addo,[3a] Berend Wassink,[3a,4] Frederick W. B. Einstein,[3b] Richard H. Jones,[3b] and Anthony C. Willis[3b,5]

Contribution from the Departments of Chemistry, The University of British Columbia, Vancouver, British Columbia, Canada V6T 1Y6, and Simon Fraser University, Burnaby, British Columbia, Canada V5A 1S6. *Received July 7, 1988*

Abstract: Electrophiles NE^+ (E = O, p-$O_2NC_6H_4N$, or S) undergo unprecedented insertions into the Cr–C σ bonds of $CpCr(NO)_2R$ complexes (Cp = η^5-C_5H_5; R = Me, CH_2SiMe_3, or Ph) to afford $[CpCr(NO)_2\{N(E)R\}]^+$ cationic complexes. Present evidence is consistent with these insertions occurring via charge-controlled, intermolecular attacks by NE^+ at the Cr–R groups in classical S_E2 processes. When R = Me and E = O, the initially formed product isomerizes intramolecularly to the novel formaldoxime complex, $[CpCr(NO)_2\{N(OH)CH_2\}]^+$, which is isolable as its PF_6^- salt. Single crystals of this salt and that resulting from the reaction of $[p\text{-}O_2NC_6H_4N_2]^+BF_4^-$ with $CpCr(NO)_2Me$ have been subjected to X-ray crystallographic analyses. $[CpCr(NO)_2\{N(OH)CH_2\}]^+PF_6^-$ crystallizes in the monoclinic space group $P2_1/c$ with cell dimensions a = 7.903 (3) Å, b = 12.192 (2) Å, c = 13.417 (5) Å, and β = 95.59 (3)°. Similarly, crystals of $[CpCr(NO)_2\{N(NC_6H_4NO_2)Me\}]^+BF_4^-$ are also monoclinic, space group $P2_1/c$, but with cell dimensions a = 8.300 (1) Å, b = 16.964 (2) Å, c = 12.536 (2) Å, and β = 101.87 (1)°. The structures of the complexes were refined to final R_F values of 0.045 and 0.054, respectively. The most chemically interesting feature of both molecular structures is that the newly formed formaldoxime and p-nitrophenylmethyldiazene ligands function as Lewis bases through nitrogen atoms toward the formally 16-electron $[CpCr(NO)_2]^+$ cations. These ligands may be displaced from the chromium's coordination sphere by the more strongly coordinating Cl^- anion. The resulting $CpCr(NO)_2Cl$ can be reconverted to $CpCr(NO)_2R$ by treatment with the appropriate Grignard or organoaluminum reagent, thereby completing a cycle by regenerating the initial organometallic reactant. The entire sequence of stoichiometric reactions forming the cycle thus constitutes a selective method for the formation of new carbon–nitrogen bonds, the net organic conversions mediated by the $CpCr(NO)_2$ group being $NE^+ + R^- \rightarrow N(E)R$.

Complexes containing σ-bonded organic ligands play a central role in transition-metal organometallic chemistry.[6] Of the various chemical properties exhibited by these complexes, probably none is more important than their ability to undergo insertion reactions

0002-7863/89/1511-2097$01.50/0

of the type

$$M\text{-}C + XY \rightarrow M\text{-}(XY)\text{-}C \quad (1)$$

where XY can be a variety of entities.[7] The particular examples of reaction 1 having XY = CO have been the most studied and are the best understood mechanistically.[7] In contrast, virtually nothing is presently known about the cases when XY = NO^+, which is isoelectronic with CO. Indeed, it was only recently that the first examples of the insertion of NO^+ into transition-metal–carbon bonds were initially communicated by us[8] and then by other investigators,[9] i.e.

$$CpCr(NO)_2CH_3 + NO^+PF_6^- \xrightarrow{CH_2Cl_2} [CpCr(NO)_2\{N(OH)CH_2\}]^+PF_6^- \quad (2)^8$$

and

$$[\{CpCo\}_3(\mu_3\text{-}\eta^1\text{-}CR)(\mu_3\text{-}\eta^1\text{-}CR')] + NO^+BF_4^- \xrightarrow{CH_3NO_2\text{-}CH_2Cl_2} [\{CpCo\}_3(\mu_3\text{-}\eta^1\text{-}CR)(\mu_3\text{-}\eta^2\text{-}C(R')=NO)]^+BF_4^- \quad (3)^9$$

where Cp = η^5-C_5H_5 and R or R′ = alkyl or aryl. Yet, reactions such as 2 and 3 are of fundamental significance since they lead to the formation of new carbon–nitrogen bonds, an intriguing goal in its own right from the viewpoint of organic synthesis.[10]

In this paper we report the extension of our previously communicated work[8] to encompass the insertions of not only the nitrosonium ion but also the thionitrosonium and aryldiazonium cations into the Cr–C σ bonds of several $CpCr(NO)_2R$ (R = alkyl or aryl complexes). Furthermore, we also present some derivative chemistry of the products resulting from insertion that has led to the development of a stoichiometric cycle for the formation of new C–N linkages, each step of the cyclic process being mediated by the $CpCr(NO)_2$ group.

Experimental Section

All reactions and subsequent manipulations were performed under anaerobic and anhydrous conditions. General procedures and instruments routinely employed in these laboratories have been described in detail previously.[12] The electrochemical cell and instrumentation employed during cyclic voltammetry studies have also been described elsewhere.[13] The commercially available reagents $Ag^+PF_6^-$ (Strem), $NO^+PF_6^-$ (Alfa), $[PPN]^+Cl^-$ (bis(triphenylphosphine)iminium chloride; Alfa), and CD_3MgI (Aldrich) were used as received without further purification.

Reaction of $CpCr(NO)_2R$ (R = Me, CD_3, CH_2SiMe_3, or Ph) with $NO^+PF_6^-$. All of these reactions were effected similarly. The experimental procedure, using $CpCr(NO)_2Me$ as a representative example, was as follows.

A green solution of $CpCr(NO)_2Me$[14a] (0.576 g, 3.00 mmol) in CH_2Cl_2 (45 mL) was treated with finely ground $NO^+PF_6^-$ (0.525 g, 3.00 mmol), and the mixture was stirred vigorously at room temperature. After 1 h, a green-brown precipitate began to form, and an IR spectrum of the supernatant solution revealed new bands at 1842 (s), 1834 (w), 1742 (s), 1734 (w), and 1710 (w) cm^{-1} in addition to the ν_{NO}'s characteristic of $CpCr(NO)_2Me$ in this solvent at 1776 and 1669 cm^{-1}. After 1.5 h, stirring was stopped, and the green-brown precipitate was permitted to settle. The green supernatant solution was removed by filter cannulation. The remaining precipitate was washed with CH_2Cl_2 (5 mL) and dried in vacuo at 20 °C (5×10^{-3} mmHg) for 1 h to obtain 0.806 g (73% yield) of a brown solid. This solid contained a mixture of the isomers $[CpCr(NO)_2\{N(O)Me\}]^+PF_6^-$ and $[CpCr(NO)_2\{N(OH)CH_2\}]^+PF_6^-$, in an approximate ratio of 2:3 as judged by its ^1H NMR spectrum.

Anal. Calcd for $C_6H_8N_3O_3PF_6Cr$: C, 19.63; H, 2.20; N, 11.45. Found: C, 19.71; H, 2.30; N, 11.33. IR (Nujol mull): ν_{OH} 3482 (s) cm^{-1}; ν_{NO} 1852 (s), 1759 (vs), 1559 (w) cm^{-1}. ^1H NMR (CD_2Cl_2, −20 °C) δ 8.92 (br s, 1 H, $H_XONCH_AH_B$), 7.66 (d, 1 H, $^2J_{H_AH_B}$ = 5.2 Hz, $H_XONCH_AH_B$), 7.14 (d, 1 H, $H_XONCH_AH_B$), 5.98 (s, 7 H, C_5H_5) 1.81 (br s, 2 H, $NOCH_3$).

Recrystallization of the brown solid from CH_2Cl_2 afforded dark green microcrystals of $[CpCr(NO)_2\{N(OH)CH_2\}]^+PF_6^-$ as the sole product. Its spectroscopic properties are the same as those exhibited by the mixture (vide supra) except for the absence of the 1559-cm^{-1} band in its IR spectrum and the methyl proton signal at δ 1.81 in its ^1H NMR spectrum.

Similar treatment of $CpCr(NO)_2CD_3$ (prepared by treating $CpCr(NO)_2Cl$[15] in Et_2O with an equimolar amount of CD_3MgI)[14b] with $NO^+PF_6^-$ in CH_2Cl_2 at room temperature for 4 h afforded green $[CpCr(NO)_2\{N(OD)CD_2\}]^+PF_6^-$ in 61% isolated yield. IR (Nujol mull): ν_{NO} 1852 (s), 1759 (vs) cm^{-1}; ν_{OD} 2581 (s) cm^{-1}. ^2H NMR (CH_3NO_2) δ 8.89 (br s, 1 D, O*D*), 7.61 (br s, 1 D, ONC*D*$_A$D$_B$), 7.25 (br s, 1 D, ONCD$_A$*D*$_B$). In the presence of even trace amounts of H_2O, the complex undergoes facile deuterium–hydrogen exchange at the OD position.

The analogous reaction between $CpCr(NO)_2CH_2SiMe_3$ (prepared by treating $CpCr(NO)_2Cl$ in Et_2O with a slight excess of Me_3SiCH_2MgCl[16]) and $NO^+PF_6^-$ in CH_2Cl_2 at room temperature for 25 min produced $[CpCr(NO)_2\{N(O)CH_2SiMe_3\}]^+PF_6^-$, which was isolated from CH_2Cl_2/hexanes as a slightly impure, viscous green oil in 81% yield.

Anal. Calcd for $C_9H_{16}N_3O_3SiPF_6Cr$: C, 24.60; H, 3.64; N, 9.57. Found: C, 23.16; H, 3.06; N, 10.00. IR (neat): ν_{NO} 1838 (s), 1736 (vs), 1628 (w) cm^{-1}. ^1H NMR (CD_2Cl_2) δ 7.80 (s, 2 H, CH_2), 5.89 (s, 5 H, C_5H_5), 0.30 (s, 9 H, $Si(CH_3)_3$).

Similarly, the stirred reaction mixture containing equimolar amounts of $CpCr(NO)_2Ph$ and $NO^+PF_6^-$ in CH_2Cl_2 at ambient temperature began to deposit red microcrystals of $[CpCr(NO)_2\{N(O)Ph\}]^+PF_6^-$ after 10 min. The precipitation was completed by the addition of hexanes, and the product salt was collected by filtration in 76% yield.

Anal. Calcd for $C_{11}H_{10}N_3O_3PF_6Cr$: C, 30.77; H, 2.33; N, 9.79. Found: C, 31.02; H, 2.29; N, 9.59. IR (Nujol mull): ν_{NO} 1850 (s), 1766 (vs), 1489 (m) cm^{-1}. ^1H NMR (CD_2Cl_2) δ 8.21–7.60 (m, 5 H, C_6H_5), 6.01 (s, 5 H, C_5H_5).

Reaction of $[CpCr(NO)_2\{N(O)CH_2SiMe_3\}]^+PF_6^-$ with H_2O. A stirred, green solution of $[CpCr(NO)_2\{N(O)CH_2SiMe_3\}]^+PF_6^-$ (0.680 g, 1.55 mmol) in CH_2Cl_2 (15 mL) was treated with 3 drops of distilled H_2O whereupon a green solid began to precipitate after ~2 min. After 45 min, the almost colorless supernatant solution was removed by filter cannulation. The remaining green solid was washed with CH_2Cl_2 (5 mL) and was dried at 20 °C (5×10^{-3} mmHg) to obtain 0.31 g (55% yield) of $[CpCr(NO)_2\{N(OH)CH_2\}]^+PF_6^-$, which was identified by its characteristic spectroscopic properties (vide supra).

Similar treatment of $[CpCr(NO)_2\{N(O)CH_2SiMe_3\}]^+PF_6^-$ with D_2O afforded a comparable yield of $[CpCr(NO)_2\{N(OD)CH_2\}]^+PF_6^-$. IR (Nujol mull): ν_{OD} 2577 (s) cm^{-1}; ν_{NO} 1852 (s), 1759 (vs), 1559 (w) cm^{-1}. ^2H NMR (CH_3NO_2) δ 8.77 (s).

Reaction of $CpCr(NO)_2Me$ with $NS^+PF_6^-$. Over a 20-min period, an orange solution of $NS^+PF_6^-$ in CH_3NO_2 (2 mmol in 30 mL, generated in situ)[17] was filter cannulated onto a stirred, olive green solution of $CpCr(NO)_2Me$ (0.384 g, 2.00 mmol) in CH_2Cl_2 (30 mL) held at 0 °C by means of an ice bath. As the reaction progressed, the reaction mixture darkened in color. The ice bath was then removed, and the mixture was allowed to warm slowly to room temperature as stirring was continued for an additional 2.5 h. Hexanes (100 mL) were then added to the final reaction mixture whereupon two immiscible liquid phases separated. The

(1) Organometallic Nitrosyl Chemistry. 38. Part 37: Legzdins, P.; Rettig, S. J.; Sánchez, L. *Organometallics* **1988**, *7*, 2394.
(2) Presented in part at the Fourth IUPAC Symposium on Organometallic Chemistry Directed Toward Organic Synthesis (OMCOS-IV), Vancouver, Canada, July 1987, Abstract PS1-50.
(3) (a) The University of British Columbia. (b) Simon Fraser University.
(4) Present address: Alberta Sulphur Research Limited, c/o Department of Chemistry, The University of Calgary, Calgary, Alberta, Canada T2N 1N4.
(5) Present address: Research School of Chemistry, Australian National University, G.P.O. Box 4, Canberra, A.C.T. 2601, Australia.
(6) Collman, J. P.; Hegedus, L. S.; Norton, J. R.; Finke, R. G. *Principles and Applications of Organotransition Metal Chemistry*; University Science Books: Mill Valley, CA, 1987.
(7) Alexander, J. J. In *The Chemistry of the Metal–Carbon Bond*; Hartley, F. R., Patai, S., Eds.; Wiley: Toronto, 1985; Vol. 2, Chapter 5.
(8) Legzdins, P.; Wassink, B.; Einstein, F. W. B.; Willis, A. C. *J. Am. Chem. Soc.* **1986**, *108*, 317.
(9) Goldhaber, A.; Vollhardt, K. P. C.; Walborsky, E. C.; Wolfgruber, M. *J. Am. Chem. Soc.* **1986**, *108*, 516.
(10) Migratory insertions of neutral nitric oxide into transition-metal–carbon bonds also result in the formation of new C–N linkages.[11]
(11) Seidler, M. D.; Bergman, R. G. *J. Am. Chem. Soc.* **1984**, *106*, 6110 and references therein.
(12) Legzdins, P.; Martin, J. T.; Oxley, J. C. *Organometallics* **1985**, *4*, 1263.
(13) Legzdins, P.; Wassink, B. *Organometallics* **1984**, *3*, 1811.
(14) (a) Hoyano, J. K.; Legzdins, P.; Malito, J. T. *J. Chem. Soc., Dalton Trans.* **1975**, 1022. (b) Piper, T. S.; Wilkinson, G. *J. Inorg. Chem.* **1956**, *3*, 104.
(15) Hoyano, J. K.; Legzdins, P.; Malito, J. T. *Inorg. Synth.* **1978**, *18*, 126.
(16) Whitmore, F. C.; Sommer, L. H. *J. Am. Chem. Soc.* **1946**, *68*, 481.
(17) Herberhold, M.; Haumaier, L. *Organomet. Synth.* **1986**, *3*, 281.

upper hexanes layer containing unreacted $CpCr(NO)_2Me$ was removed by cannulation and discarded. Solvent was removed from the lower nitromethane layer in vacuo to obtain a viscous green oil. Trituration of this oil with CH_2Cl_2 (10 mL) resulted in the formation of 0.31 g (40% yield) of a green powder, which was formulated as $[CpCr(NO)_2\{(NSH)CH_2\}]^+PF_6^-$ on the basis of its IR spectrum. IR (Nujol mull): ν_{NH} 3331 (s) cm^{-1}; ν_{NO} 1829 (s), 1723 (vs) cm^{-1}. Unfortunately, this green powder was unstable, decomposing even when maintained at −20 °C overnight. Consequently, a consistent elemental analysis of this material could not be obtained.

Reaction of $CpCr(NO)_2Me$ with $[p\text{-}O_2NC_6H_4N_2]^+BF_4^-$. The *p*-nitrophenyldiazonium salt, $[p\text{-}O_2NC_6H_4N_2]^+BF_4^-$ (0.474 g, 2.00 mmol),[18] was dissolved in CH_3NO_2 (50 mL), and the resulting light orange solution was transferred dropwise by cannula onto a stirred CH_2Cl_2 (50 mL) solution of $CpCr(NO)_2Me$ (0.384 g, 2.00 mmol) at ambient temperature. The reaction mixture was stirred for a total of 2 h, during which time the originally green solution became red, and IR monitoring revealed replacement of the original ν_{NO}'s at 1777 and 1669 cm^{-1} by new bands at 1846 and 1746 cm^{-1}. Solvent was removed from the final mixture in vacuo, and the remaining oily residue was reprecipitated from CH_2Cl_2–hexanes. Trituration of the oil thus obtained with CH_2Cl_2 afforded a green-brown microcrystalline solid and a red supernatant solution. The crystals were collected by filtration, washed quickly with CH_2Cl_2 (2 × 5 mL), and dried at 20 °C (5 × 10^{-3} mmHg) for 1 h to obtain 0.212 g (25% yield) of analytically pure $[CpCr(NO)_2\{N(NC_6H_4NO_2)Me\}]^+BF_4^-$.

Anal. Calcd for $C_{12}H_{12}O_4N_5BF_4Cr$: C, 33.58; H, 2.80; N, 16.32. Found: C, 33.44; H, 2.87; N, 16.20. IR (Nujol mull): ν_{NO} 1833 (s), 1726 (vs) cm^{-1}; also 1605 (m), 1590 (m), 1560 (w) cm^{-1}. ^1H NMR (CD_3NO_2) δ 8.43 (d, 2 H, *m-H*, $^3J_{H_AH_X}$ = 9.3 Hz), 7.29 (d, 2 H, *o-H*), 6.12 (s, 5 H, C_5H_5), 4.26 (s, 3 H, CH_3). Definitive assignment of the ν_{NN} of the diazene ligand in the IR spectrum requires a proper ^{15}N-labeling study.

Reaction of $[CpCr(NO)_2\{N(O)Ph\}]^+PF_6^-$ with $[PPN]^+Cl^-$. To a stirred, red solution of $[CpCr(NO)_2\{N(O)Ph\}]^+PF_6^-$ (0.268 g, 0.625 mmol) in CH_2Cl_2 (25 mL) at ambient temperature was added a slight excess of $[PPN]^+Cl^-$ (0.40 g, 0.70 mmol) whereupon the solution immediately became green. After 1 min, an IR spectrum of this solution was devoid of absorptions due to the nitrosobenzene-containing complex but did exhibit strong bands attributable to $CpCr(NO)_2Cl$ (ν_{NO} 1817 (s), 1711 (vs) cm^{-1}) and uncomplexed PhNO (1506, 1439 cm^{-1}). Removal of solvent from the final reaction mixture in vacuo and sublimation of the residue at 20 °C (5 × 10^{-3} mmHg) onto a dry-ice-cooled probe produced 0.02 g (34% yield) of PhNO, which was identified by comparison of its spectroscopic properties with those exhibited by an authentic sample. The relatively low isolated yield of PhNO from this clean (by IR) conversion was undoubtedly a reflection of the nitroso compound's considerable volatility.

Sequential Treatment of $CpCr(NO)_2Ph$ with $[p\text{-}O_2NC_6H_4N_2]^+BF_4^-$ and $[PPN]^+Cl^-$. A stirred, green solution of $CpCr(NO)_2Ph$ (0.31 g, 1.2 mmol) in CH_3NO_2 (5 mL) at room temperature was treated with solid $[p\text{-}O_2NC_6H_4N_2]^+BF_4^-$ (0.24 g, 1.0 mmol) whereupon the reaction mixture became red-brown within 10 min. After 5 h, the reaction mixture was filtered through a medium-porosity glass frit, and solvent was removed from the filtrate in vacuo. The remaining brown residue was dissolved in CH_2Cl_2 (40 mL), $[PPN]^+Cl^-$ (0.63 g, 1.1 mmol) was added, and the resulting solution was stirred for 15 min whereupon it became green-orange in color. The final reaction mixture was taken to dryness under reduced pressure, and the residue thus obtained was extracted with hexanes (2 × 70 mL) to leave behind a green-brown powder. Solvent was removed from the combined orange extracts in vacuo, the resulting residue was dissolved in Et_2O (10 mL), and this solution was transferred to the top of an alumina column (Woelm neutral, activity 1, 2 × 10 cm) made up in Et_2O. Elution of the column in air with Et_2O developed a single orange band, which was eluted from the column and collected. Solvent removal from the eluate in vacuo afforded an orange solid, which was recrystallized from hexanes to obtain 0.08 g (35% yield) of *p*-$O_2NC_6H_4N_2Ph$ as an orange microcrystalline solid.

Anal. Calcd for $C_{12}H_9N_3O_2$: C, 63.43; H, 3.99; N, 18.49. Found: C, 63.50; H, 4.01, N, 18.44. Low-resolution mass spectrum (probe temperature 150 °C): *m/z* 227 (P^+).

The green-brown powder remaining after the hexanes extraction was recrystallized from CH_2Cl_2–hexanes to obtain 0.16 g (75% yield) of golden $CpCr(NO)_2Cl$, which was readily identifiable by its characteristic IR and mass spectra.[15]

Crystal Structure Analysis of $[CpCr(NO)_2\{N(OH)CH_2\}]^+PF_6^-$. Single crystals of $[CpCr(NO)_2\{N(OH)CH_2\}]^+PF_6^-$ suitable for X-ray crystallographic analysis were grown by maintaining a concentrated CH_2Cl_2 solution of the salt at −20 °C for 2 days. A dark green needle of the complex was sealed in a thin-walled glass capillary while maintaining an atmosphere of dry dinitrogen throughout. The crystal was mounted on an Enraf-Nonius CAD4-F diffractometer, and accurate cell dimensions and the orientation matrix were determined by least-squares analysis of the setting angles of 25 reflections with 28.6° < 2θ < 36.7°, which were accurately centered. Crystal data are given in Table I.

Table I. Crystal Data for $[CpCr(NO)_2\{N(OH)CH_2\}]^+PF_6^-$ and $[CpCr(NO)_2\{N(NC_6H_4NO_2)Me\}]^+BF_4^-$

	$[CpCr(NO)_2\{N(OH)CH_2\}]^+PF_6^-$	$[CpCr(NO)_2\{N(NC_6H_4NO_2)Me\}]^+BF_4^-$
formula	$C_6H_8N_3O_3F_6PCr$	$C_{12}H_{12}N_5O_4F_4BCr$
formula wt	367.12	428.14
cryst syst	monoclinic	monoclinic
space gp	$P2_1/c$	$P2_1/c$
a, Å	7.903 (3)	8.300 (1)
b, Å	12.192 (2)	16.964 (2)
c, Å	13.417 (5)	12.536 (2)
β, deg	95.59 (3)	101.87 (1)
V, Å^3	1286.6	1727.3
Z	4	4
ρ_{calcd}, g cm^{-3}	1.895	1.650
μ, cm^{-1}	10.71	7.13

Table II. Data Collection and Refinement for $[CpCr(NO)_2\{N(OH)CH_2\}]^+PF_6^-$ and $[CpCr(NO)_2\{N(NC_6H_4NO_2)Me\}]^+BF_4^-$

	$[CpCr(NO)_2\{N(OH)CH_2\}]^+PF_6^-$	$[CpCr(NO)_2\{N(NC_6H_4NO_2)Me\}]^+BF_4^-$
diffractometer	Enraf-Nonius CAD4-F	
radiatn	Mo Kα, graphite monochromator	
λ of radiatn, Å	0.709 30 (α_1); 0.713 59 (α_2)	
scan mode	coupled ω–2θ	
scan width	(0.85 + 0.35 tan θ)° in ω	(0.95 + 0.35 tan θ)° in ω
scan speed	3.29–0.78° min^{-1} in ω	2.75–0.75° min^{-1} in ω
bckgd	scan extended by 25% on each side	
2θ range	0–50°	
size of cryst, mm	0.15 × 0.18 × 0.53	0.43 × 0.14 × 0.16
total no. of reflctns	2258	3020
obsd reflctns	1262[a]	1741[b]
no. of variables	193	244
final R_F[c,d]	0.045	0.054
final R_{wF}[e,d]	0.050	0.055
GOF[f,d]	1.79	1.25
p (wt scheme)	0.0004	0.0008

[a] Reflections with $I > 3\sigma(I)$. [b] Reflections with $I > 1.5\sigma(I)$. [c] $R_F = \sum||F_o| - |F_c||/\sum|F_o|$. [d] Observed reflections only. [e] $R_{wF} = [\sum w(|F_o| - |F_c|)^2/\sum w|F_o|^2]^{1/2}$. [f] GOF = $[\sum w(|F_o| - |F_c|)^2/(\text{no. observations} - \text{no. variables})]^{1/2}$.

The intensities of a unique data set (h, −9 → 9; k, 0 → 14; l, 0 → 15) were collected as outlined in Table II. Two standard reflections, measured at intervals of 90 min of exposure time, showed small (<3%) variations from their mean. The data were thus scaled according to a curve derived by five-point smoothing from the standard reflections. L_p and absorption corrections (T = 0.826–0.863) were also applied to the data.[19]

The structure was solved by standard heavy-atom techniques, which located all non-hydrogen atoms. Least-squares refinement of these atoms, initially with isotropic and then with anisotropic temperature factors and with the cyclopentadienyl H atoms fixed at calculated positions (r_{C-H} = 0.95 Å; U_H = average U_{eq} of Cp C atoms), yielded R = 0.061. At this stage, the hydrogen atoms of the formaldoxime ligand were located in a difference electron density map. This model, however, exhibited two unsatisfactory aspects, namely: (1) the four fluorine atoms F(3)–F(6), comprising a square plane, displayed very anisotropic motion, and large peaks were situated between them in the difference electron density map; and (2) the cyclopentadienyl carbon atoms also exhibited very anisotropic motion in addition to short C–C distances (~1.33 Å). These features suggested disorder of the respective entities, and so the model was modified to allow for this disorder. Specifically, within the PF_6^- anion, the four atoms F(3)–F(6) were assigned occupancies of n (initially 0.8) and individual isotropic temperature factors, and four new fluorine atoms, F(34)–F(63), of occupancy 1 − n were placed between them and were assigned one common isotropic temperature factor. For the cyclo-

(18) Balz, G.; Schiemann, G. *Chem. Ber.* **1927**, *60*, 1186.

(19) DeMeulenaer, J.; Tompa, H. *Acta Crystallogr.* **1965**, *19*, 1014.

Table III. Final Atomic Coordinates and Temperature Factors (Å^2 × 10^3) of the Non-Hydrogen Atoms of $[CpCr(NO)_2\{N(OH)CH_2\}]^+PF_6^-$

atom	x	y	z	U_{eq} or U
Cr	0.23339 (11)	0.36899 (8)	0.32377 (7)	40[a]
N(1)	0.2037 (6)	0.2033 (4)	0.3241 (4)	53[a]
O(1)	0.0807 (8)	0.1548 (4)	0.2569 (5)	79[a]
C(1)	0.2848 (12)	0.1330 (8)	0.3775 (7)	76[a]
N(2)	0.2744 (7)	0.3830 (5)	0.4500 (4)	62[a]
O(2)	0.3027 (7)	0.4017 (5)	0.5350 (4)	88[a]
N(3)	0.0237 (7)	0.4032 (4)	0.3244 (4)	53[a]
O(3)	-0.1111 (6)	0.4384 (4)	0.3268 (5)	76[a]
C(11)[b]	0.431 (3)	0.341 (1)	0.221 (1)	51[c]
C(12)[b]	0.491 (2)	0.415 (2)	0.295 (1)	51[c]
C(13)[b]	0.383 (3)	0.510 (1)	0.287 (1)	51[c]
C(14)[b]	0.261 (2)	0.490 (2)	0.206 (2)	51[c]
C(15)[b]	0.285 (2)	0.385 (2)	0.166 (1)	51[c]
C(21)[b]	0.479 (2)	0.362 (2)	0.258 (2)	51[c]
C(22)[b]	0.457 (2)	0.467 (2)	0.297 (1)	51[c]
C(23)[b]	0.312 (3)	0.517 (1)	0.247 (2)	51[c]
C(24)[b]	0.243 (2)	0.444 (2)	0.174 (1)	51[c]
C(25)[b]	0.348 (3)	0.349 (1)	0.180 (1)	51[c]
P(1)	-0.2051 (2)	0.2781 (2)	0.0291 (1)	55[a]
F(1)	-0.2357 (7)	0.2750 (4)	-0.0871 (3)	103[a]
F(2)	-0.1734 (7)	0.2817 (5)	0.1469 (3)	106[a]
F(3)[d]	-0.086 (2)	0.1783 (12)	0.0323 (7)	119[a]
F(4)[d]	-0.059 (2)	0.3605 (15)	0.0143 (9)	150[a]
F(5)[d]	-0.327 (1)	0.3817 (8)	0.0300 (5)	107[a]
F(6)[d]	-0.361 (1)	0.2070 (9)	0.0422 (7)	117[a]
F(34)[d]	-0.020 (3)	0.247 (2)	0.028 (2)	78[e]
F(45)[d]	-0.153 (3)	0.392 (2)	0.041 (1)	78[e]
F(56)[d]	-0.388 (2)	0.307 (2)	0.027 (1)	78[e]
F(63)[d]	-0.242 (3)	0.151 (2)	0.020 (1)	78[e]

[a] U_{eq} is the cube root of the product of the principal axes of the ellipsoid. [b] Occupancy refined. For C(11)–C(15), occ = 0.503; C(21)–C(25), occ = 0.497. This occ parameter has an esd of 0.009. [c] One isotropic thermal parameter was refined for all of C(11)–C(25); U = 0.051 (1) Å^2. [d] Occupancy refined. For F(3)–F(6), occ = 0.75; F(34)–F(63), occ = 0.25. This occ parameter has an esd of 0.02. [e] One isotropic thermal parameter was refined for all of F(34)–F(63): U = 0.078 (6) Å^2.

pentadienyl ring, each carbon atom was split tangentially into two atoms of occupancy 0.5 to form two interleaved five-membered rings, one of occupancy m and the other $1 - m$. One isotropic temperature factor was refined for all 10 half-atoms. Hydrogen atoms of occupancy m or $1 - m$, riding on the cyclopentadienyl C atoms, were given one isotropic temperature factor. Similarly, H(1) and H(2), the methylene hydrogen atoms of the formaldoxime ligand, were given one isotropic temperature factor. H(10), the hydroxyl hydrogen atom of the $N(OH)CH_2$ group, was given the fixed value of U = 0.10 Å^2. Initially, "soft" constraints[20] of P–F = 1.55 Å and F–P–F = 180 or 90° were applied to F(34)–F(63), and C–C = 1.39 Å and all five sites planar were applied to each cyclopentadienyl ring in full-matrix refinement. Later, F(3)–F(6) were assigned individual anisotropic temperature factors, and finally the constraints were removed. The significant improvement in R to 0.045, a generally featureless final difference electron density map (all peaks <0.33 e Å^{-3}), and the more reasonable bond distances confirm the superiority of the final model over that in which disorder had not been taken into account.

Refinement throughout was by full-matrix least-squares minimizing the function $\sum w(|F_o| - |F_c|)^2$ in which w was initially unity, but in later cycles $w = [\{\sigma(F_o)\}^2 + pF_o^2]^{-1}$ where $\sigma(F_o)$ is from the counter statistics. In the final cycle of refinement all shift to error ratios were <0.01. Neutral-atom scattering factors with anomalous dispersion corrections were used.[21] The computations were performed on a VAX 11-750 computer using the NRC VAX crystal structure package[22] and the CRYSTALS suite of programs.[23]

(20) Waser, J. *Acta Crystallogr.* **1963**, *16*, 1091.
(21) *International Tables for X-ray Crystallography*; Kynoch Press: Birmingham, England, 1974; Vol. IV, Tables 2.2B and 2.3.1.
(22) (a) Larson, A. C.; Gabe, E. J. In *Computing in Crystallography*; Schenk, H., Olthof-Hazekamp, R., Van Koningsveld, H., Bassi, G. C., Eds.; Delft University Press: Delft, Holland, 1978; p 81. (b) Larson, A. C.; Lee, F. L.; LePage, Y.; Gabe, E. J. *The NRC VAX Crystal Structure System*; Chemistry Division, National Research Council; Ottawa, Canda, 1984.
(23) Watkin, D. J.; Carruthers, J. R.; Betteridge, P. W. *CRYSTALS User Guide*; Chemical Crystallography Laboratory, University of Oxford: Oxford, U.K., 1985.

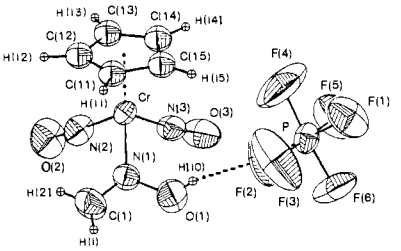

Figure 1. Solid-state molecular structure of $[CpCr(NO)_2\{N(OH)CH_2\}]^+PF_6^-$. Only one orientation of the disordered Cp and PF_6^- groups is shown.

Table IV. Important Interatomic Distances (Å) and Angles (deg) for $[CpCr(NO)_2\{N(OH)CH_2\}]^+PF_6^-$[a]

Cr–N(1)	2.034 (5)	Cr–N(3)	1.709 (5)
Cr–N(2)	1.702 (6)	Cr···CP	1.843
Cr–C(11)	2.212 (14)	Cr–C(21)	2.207 (14)
Cr–C(12)	2.179 (14)	Cr–C(22)	2.195 (14)
Cr–C(13)	2.167 (14)	Cr–C(23)	2.191 (14)
Cr–C(14)	2.187 (14)	Cr–C(24)	2.216 (14)
Cr–C(15)	2.202 (14)	Cr–C(25)	2.217 (14)
N(1)–C(1)	1.253 (9)	N(2)–O(2)	1.163 (6)
N(1)–O(1)	1.392 (7)	N(3)–O(3)	1.152 (6)
C(1)–H(1)	0.83 (7)	O(1)–H(10)	0.72 (8)
C(1)–H(2)	0.88 (7)		
C(11)–C(12)	1.39 (2)	C(21)–C(22)	1.40 (2)
C(12)–C(13)	1.44 (2)	C(22)–C(23)	1.40 (2)
C(13)–C(14)	1.41 (2)	C(23)–C(24)	1.39 (2)
C(14)–C(15)	1.40 (2)	C(24)–C(25)	1.42 (2)
C(15)–C(11)	1.41 (2)	C(25)–C(21)	1.40 (2)
P(1)–F(1)	1.555 (5)	P(1)–F(34)	1.51 (3)
P(1)–F(2)	1.577 (5)	P(1)–F(45)	1.46 (2)
P(1)–F(3)	1.539 (8)	P(1)–F(56)	1.48 (2)
P(1)–F(4)	1.560 (8)	P(1)–F(63)	1.58 (2)
P(1)–F(5)	1.589 (7)		
P(1)–F(6)	1.533 (7)		
H(10)···F(2)	2.14 (8)	O(1)···F(2)	2.833 (7)

CP–Cr–N(1)	117 (6)	N(1)–Cr–N(2)	96.2 (3)
CP–Cr–N(2)	123.4	N(1)–Cr–N(3)	97.5 (2)
CP–Cr–N(3)	122.3	N(2)–Cr–N(3)	93.5 (3)
Cr–N(1)–C(1)	128.9 (5)	Cr–N(2)–O(2)	174.5 (6)
Cr–N(1)–O(1)	119.6 (4)	Cr–N(3)–O(3)	172.1 (5)
C(1)–N(1)–O(1)	111.5 (6)	C(25)–C(21)–C(22)	105.6 (12)
C(15)–C(11)–C(12)	109.2 (12)	C(21)–C(22)–C(23)	110.2 (12)
C(11)–C(12)–C(13)	108.2 (11)	C(22)–C(23)–C(24)	107.9 (12)
C(12)–C(13)–C(14)	105.6 (12)	C(23)–C(24)–C(25)	106.7 (11)
C(13)–C(14)–C(15)	110.4 (12)	C(24)–C(25)–C(21)	109.6 (12)
C(14)–C(15)–C(11)	106.5 (12)	N(1)–O(1)–H(10)	111 (7)
N(1)–C(1)–H(1)	125 (5)	O(1)–H(10)···F(2)	162 (10)
N(1)–C(1)–H(2)	117 (5)	P–F(2)···H(10)	122 (3)
H(1)–C(1)–H(2)	118 (8)		

[a] CP is the centroid of C(11)–C(15) and C(21)–C(25) (0.3691, 0.4280, 0.2332).

Final positional and isotropic (or equivalent isotropic) thermal parameters for the non-hydrogen atoms are presented in Table III, and selected distances and angles involving these atoms are tabulated in Table IV. Coordinates of the hydrogen atoms, anisotropic thermal parameters, additional distances and angles, least-squares planes, and structure factors are given in Tables V–IX and are deposited as supplementary material. A thermal ellipsoid plot[24] of the solid-state molecular structure of $[CpCr(NO)_2\{N(OH)CH_2\}]^+PF_6^-$ is shown in Figure 1, the atoms being labeled as indicated.

Crystal Structure Analysis of $[CpCr(NO)_2\{N(NC_6H_4NO_2)Me\}]^+BF_4^-$. Single crystals of this salt suitable for X-ray crystallographic analysis were grown by maintaining a saturated CH_2Cl_2 solution of the complex under N_2 at -20 °C for 3 days. An olive green, brick-shaped crystal of $[CpCr(NO)_2\{N(NC_6H_4NO_2)Me\}]^+BF_4^-$ was mounted and sealed in a thin-walled glass capillary under dinitrogen. The crystal was then transferred to the diffractometer, and the unit cell parameters and an

(24) Davies, E. K. *SNOOPI Plot Program*; Chemical Crystallography Laboratory, University of Oxford: Oxford, U.K., 1984.

Table X. Final Atomic Coordinates and Equivalent Isotropic Thermal Parameters of the Non-Hydrogen Atoms of $[CpCr(NO)_2\{N(NC_6H_4NO_2)Me\}]^+BF_4^-$

atom	*x*	*y*	*z*	B_{eq}[a]
Cr	0.24532 (10)	0.16201 (5)	0.12702 (7)	3.10
N(1)	0.1537 (6)	0.1992 (3)	0.2265 (4)	4.3
N(2)	0.3060 (6)	0.2507 (3)	0.0861 (4)	4.8
N(3)	0.4621 (5)	0.1319 (2)	0.2309 (3)	3.3
N(4)	0.4551 (5)	0.1067 (3)	0.3214 (3)	3.8
N(5)	0.9943 (7)	0.0410 (5)	0.6628 (4)	6.2
O(1)	0.0773 (6)	0.2229 (3)	0.2865 (4)	8.1
O(2)	0.3327 (7)	0.3110 (3)	0.0485 (4)	8.4
O(3)	1.0774 (7)	0.0963 (4)	0.7049 (4)	9.1
O(4)	1.0192 (6)	−0.0270 (4)	0.6909 (4)	8.1
C(1)	1.1635 (8)	0.0395 (3)	0.1004 (5)	4.2
C(2)	0.2741 (8)	0.0546 (3)	0.0342 (5)	4.3
C(3)	0.2110 (8)	0.1334 (4)	−0.0399 (4)	4.7
C(4)	0.0574 (8)	0.1362 (3)	−0.0178 (5)	4.5
C(5)	0.0276 (7)	0.0890 (4)	0.0686 (5)	4.4
C(6)	0.6214 (7)	0.1436 (4)	0.1978 (5)	5.5
C(7)	0.6032 (6)	0.0907 (3)	0.4025 (4)	3.5
C(8)	0.6867 (8)	0.1518 (3)	0.4613 (5)	4.8
C(9)	0.8149 (8)	0.1358 (4)	0.5465 (5)	5.1
C(10)	0.8539 (7)	0.0586 (4)	0.5709 (4)	4.3
C(11)	0.7725 (7)	−0.0036 (4)	0.5147 (5)	4.3
C(12)	0.6424 (7)	0.0132 (4)	0.4277 (4)	4.1
B	0.5855 (10)	0.3590 (4)	0.3329 (6)	4.7
F(1)	0.4644 (5)	0.3021 (2)	0.3104 (3)	7.2
F(2)	0.6459 (5)	0.3611 (2)	0.4424 (3)	7.3
F(3)	0.5150 (7)	0.4296 (3)	0.3044 (5)	11.2
F(4)	0.7066 (7)	0.3442 (5)	0.2842 (4)	14.4

[a] B_{eq} is the arithmetic mean of the principal axes of the thermal ellipsoid.

orientation matrix were obtained from the accurate setting angles of 25 reflections ($15° < 2\theta < 31°$). Crystal data are presented in Table I. Data were collected as summarized in Table II and were corrected for Lorentz and polarization, but not absorption, effects. Two reflections measured every 1 h showed a slight decrease in intensity (2%) over the course of data collection, and the data were thus scaled appropriately.

The structure was solved by conventional heavy-atom methods and refined by full-matrix least squares. The positions of the hydrogen atoms were located in difference Fourier syntheses and were not refined. Similar hydrogen atoms were assigned the same temperature factor; all non-hydrogen atoms were refined anisotropically. The refinement was considered to be complete when the ratio of calculated shifts to esd's was less than 0.1. During the final cycles of refinement, the weighting scheme employed was $w = [\{\sigma(F_o)\}^2 + pF_o^2]^{-1}$. The largest peak in the final difference electron density map was of height 0.33 (8) e Å^{-3} and was situated 1.27 Å from the boron atom. This observation, taken together with the uneven distribution of the fluorine temperature factors, may be indicative of some residual disorder of the BF_4^- anion. Complex neutral-atom scattering factors were used,[21] and computer programs[22,23] were run on an in-house VAX 11-750.

Final atomic coordinates and equivalent isotropic thermal parameters of the non-hydrogen atoms of the complex are given in Table X, and selected bond distances and interbond angles are listed in Table XI. Tables of hydrogen atom coordinates and temperature factors, anisotropic thermal parameters, and observed and calculated structure factors (Tables XII–XIV) are available as supplementary material. Two views of the thermal ellipsoid plot[24] of the solid-state molecular structure of the $[CpCr(NO)_2\{N(NC_6H_4NO_2)Me\}]^+$ cation showing non-hydrogen atoms only are presented in Figure 2, the atoms being labeled as indicated.

Results and Discussion

Insertions of the Nitrosonium Ion into Chromium–Carbon σ Bonds. Treatment of various $CpCr(NO)_2R$ complexes (R = alkyl or aryl) with NO^+ results in the clean insertion of the nitrosonium ion into the Cr–C σ bonds, i.e.

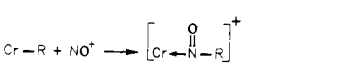

(4)

the cationic products resulting from transformations 4 generally being isolable in good yields as their PF_6^- salts. In the special case when R = Me, the insertion first generates a brown complex whose spectroscopic properties are consistent with it containing the $[CpCr(NO)_2\{N(O)Me\}]^+$ cation. Specifically, its IR spectrum

Table XI. Selected Bond Lengths (Å) and Angles (deg) for $[CpCr(NO)_2\{N(NC_6H_4NO_2)Me\}]^+BF_4^-$

Cr–N(1)	1.709 (5)	Cr–N(2)	1.699 (5)
Cr–N(3)	2.057 (4)	Cr–C(1)	2.191 (5)
Cr–C(2)	2.201 (5)	Cr–C(3)	2.212 (5)
Cr–C(4)	2.181 (5)	Cr–C(5)	2.189 (5)
N(1)–O(1)	1.152 (7)	N(2)–O(2)	1.167 (7)
N(3)–N(4)	1.225 (6)	N(3)–C(6)	1.478 (7)
N(4)–C(7)	1.450 (6)	C(7)–C(12)	1.375 (8)
C(7)–C(8)	1.374 (8)	C(12)–C(11)	1.397 (8)
C(11)–C(10)	1.368 (9)	C(8)–C(9)	1.371 (8)
C(9)–C(10)	1.368 (10)	C(10)–N(5)	1.490 (7)
N(5)–O(3)	1.218 (11)	N(5)–O(4)	1.213 (11)
C(1)–C(2)	1.383 (9)	C(2)–C(3)	1.389 (9)
C(3)–C(4)	1.413 (10)	C(4)–C(5)	1.409 (9)
C(5)–C(1)	1.396 (9)		
N(1)–Cr–N(2)	95.6 (3)	N(1)–Cr–N(3)	95.3 (2)
N(2)–Cr–N(3)	97.8 (2)	Cr–N(1)–O(1)	173.2 (5)
Cr–N(2)–O(2)	172.4 (5)	Cr–N(3)–C(6)	120.4 (3)
Cr–N(3)–N(4)	118.1 (3)	N(4)–N(3)–C(6)	121.5 (4)
N(3)–N(4)–C(7)	121.3 (4)	N(4)–C(7)–C(12)	117.8 (5)
N(4)–C(7)–C(8)	119.7 (5)	C(12)–C(7)–C(8)	121.9 (5)
C(7)–C(12)–C(11)	118.9 (5)	C(12)–C(11)–C(10)	117.7 (5)
C(11)–C(10)–C(9)	123.7 (5)	C(10)–C(9)–C(8)	118.3 (6)
C(7)–C(8)–C(9)	119.6 (5)	C(11)–C(10)–N(5)	117.9 (6)
C(9)–C(10)–N(5)	118.4 (6)	C(10)–N(5)–O(3)	117.7 (7)
C(10)–N(5)–O(4)	118.3 (7)	O(3)–N(5)–O(4)	124.0 (6)
C(1)–C(2)–C(3)	109.2 (5)	C(2)–C(3)–C(4)	107.3 (5)
C(3)–C(4)–C(5)	107.6 (5)	C(4)–C(5)–C(1)	107.6 (5)
C(5)–C(1)–C(2)	108.3 (5)		

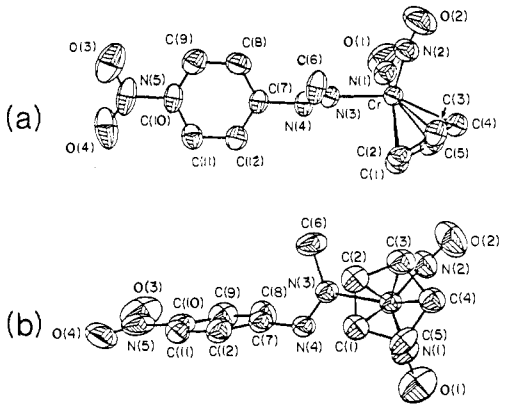

Figure 2. Views of the molecular structure of the $[CpCr(NO)_2\{N(NC_6H_4NO_2)Me\}]^+$ cation: (a) approximately parallel to the Cp ligand and (b) approximately perpendicular to the Cp ligand. Only non-hydrogen atoms are shown.

(Nujol mull) exhibits a band at 1559 cm^{-1} and its ^{1}H NMR spectrum (CD_2Cl_2, −20 °C) displays a singlet at δ 1.81, both features being attributable to the nitrosomethane ligand.[25] In solutions, however, this brown complex isomerizes irreversibly to a novel formaldoxime complex, i.e.

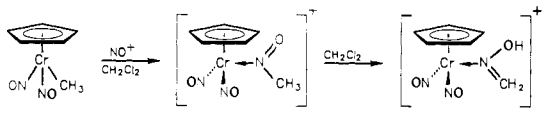

(5)

The isomerization step depicted in eq 5 is rapid in poorly coordinating solvents such as CH_2Cl_2 and CH_3NO_2,[26] and the final green formaldoxime complex, $[CpCr(NO)_2\{N(OH)CH_2\}]^+PF_6^-$, is best isolated by crystallization from CH_2Cl_2. In the solid state, the latter salt may be handled in air for short periods of time, but it is best stored under dry N_2.

A single-crystal X-ray crystallographic analysis of $[CpCr(NO)_2\{N(OH)CH_2\}]^+PF_6^-$ (the essential details of which are summarized in Tables I and II) establishes that the organometallic

(25) For comparison, free MeNO exhibits a ν_{NO} of 1564 cm^{-1}. See: Feuer, H. *The Chemistry of the Nitroso and Nitro Groups*; Wiley-Interscience: Toronto, 1969; Vol. 1, p 140.

(26) Drago, R. S. *Pure Appl. Chem.* **1980**, *52*, 2261.

cation possesses a normal "three-legged piano stool" molecular structure. A thermal ellipsoid plot of this structure is shown in Figure 1, and pertinent intramolecular dimensions are tabulated in Table IV. Within the cation, the $CpCr(NO)_2$ fragment is normal, closely resembling that found in $CpCr(NO)_2Cl$.[27] The $CrN(OH)CH_2$ portion of the cation is essentially planar, and the intramolecular dimensions of the formaldoxime ligand resemble those of free formaldoxime.[28] Consequently, in valence-bond terms, the bonding within this grouping is representable as

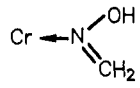

with the formaldoxime ligand functioning as a formal two-electron donor to the metal center. The hydroxyl H atom of this ligand is also linked by a hydrogen bond to the PF_6^- counteranion[29] [H(10)–F(2) = 2.14 (8) Å, represented by the dashed line in Figure 1]. The spectroscopic properties of $[CpCr(NO)_2\{N(OH)CH_2\}]^+PF_6^-$ can be readily understood in terms of its solid-state molecular structure, thereby indicating that the basic structural units persist in solutions. For instance, the ^1H NMR spectrum of the salt in CD_2Cl_2 exhibits a broad singlet at δ 8.92 and AB patterns at δ 7.66 and 7.14 attributable to the hydroxyl and methylene protons, respectively, of the formaldoxime ligand.

The reaction between the perdeuteriomethyl complex, $CpCr(NO)_2CD_3$, and NO^+ apparently proceeds in a manner analogous to that shown in eq 5. In this instance, the final green salt, $[CpCr(NO)_2\{N(OD)CD_2\}]^+PF_6^-$, is isolable in 61% yield. The occurrence of this conversion thus verifies that the hydroxyl H atom of the formaldoxime ligand in reaction 5 does indeed originate from the methyl group in the organometallic reactant and not from some other source such as the solvent. The presence of the perdeuterated formaldoxime ligand in the final complex is clearly evident in its IR [Nujol mull: ν_{OD} 2581 cm^{-1}; ν_{OH}/ν_{OD} (calcd) 1.37, (found) 1.35] and ^2H NMR [CH_3NO_2; three singlets of equal intensity at δ 8.89, 7.61, and 7.25] spectra. However, this ligand undergoes facile deuterium–hydrogen exchange at the OD position in the presence of even trace amounts of H_2O.

When R = CH_2SiMe_3 in the general transformation 4, the NO^+ inserted product can be precipitated as its PF_6^- salt by the addition of hexanes to the final reaction mixture. Isolated in this manner, the complex is a slightly impure, dark green tar, which exhibits IR and ^1H NMR spectra (see the Experimental Section for details) that are completely consistent with its cation possessing the molecular structure shown in the middle of eq 6. Also as indicated

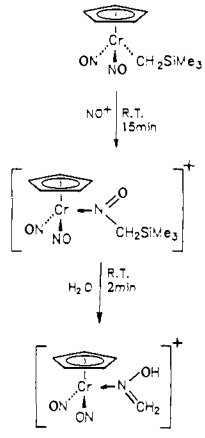

(6)

in eq 6, this cation is readily hydrolyzed to the ubiquitous formaldoxime-containing complex. Interestingly, if D_2O rather than H_2O is employed to effect the second step of reaction 6, the final product displays deuterium incorporation solely at the hydroxyl position, i.e.

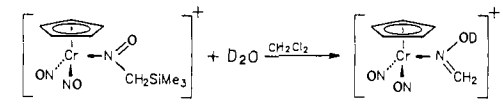

(7)

This latter observation is indicative of the hydrolysis reaction proceeding so as to afford the formaldoxime complex directly, e.g.

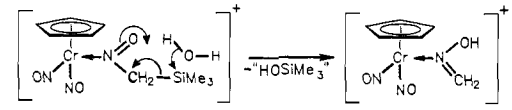

(8)

Had the cleavage of the C–Si link by D_2O proceeded so as to generate initially the CH_2DNO-containing cation, which would then isomerize to the final product (eq 5), a distribution of the deuterium label among the hydroxyl and methylene sites of the formaldoxime ligand would have been observed. For comparison, it may be noted that the analogous carbon–silicon bond in the neutral $CpCr(NO)_2CH_2SiMe_3$ reactant is much less prone to cleavage. Thus, the complex is inert to H_2O and MeOH, and I_2 cleanly breaks the Cr–C bond instead to produce $CpCr(NO)_2I$.

Finally, the NO^+ insertion reaction (eq 4) can also be extended to encompass chromium–aryl linkages as well. For instance, treatment of $CpCr(NO)_2Ph$ with $NO^+PF_6^-$ in CH_2Cl_2 affords the $[CpCr(NO)_2\{N(O)Ph\}]^+PF_6^-$ product, which is isolable in 76% yield as a red, microcrystalline solid. This nitrosobenzene complex is very soluble under ambient conditions in noncoordinating solvents such as CH_2Cl_2 and CH_3NO_2[26] but can be crystallized from them at −20 °C. The physical and spectroscopic properties of the complex are fully in accord with its cation having a piano stool molecular structure. In particular, the fact that the ν_{NO} exhibited by the PhNO ligand is 17 cm^{-1} lower than in the free state is indicative of it being coordinated in a monodentate fashion through N.[30]

Possible Mechanisms for the Nitrosonium Insertion Reactions. The two most likely mechanistic pathways for the unprecedented reactions 4 are those involving either oxidatively induced, intramolecular insertion of bound NO into the Cr–C σ bonds or charge-controlled, intermolecular attacks by NO^+ at the Cr–R groups. Each pathway is next considered in some detail.

(a) Oxidatively Induced Migratory Insertion of Bound NO. Ample evidence exists in the chemical literature that during its reactions with organometallic substrates the nitrosonium cation may, on occasion, simply function as a 1-electron oxidant.[31] Hence, it is conceivable that the insertion reactions 4 may well proceed in the manner summarized in eq 9. As indicated, the

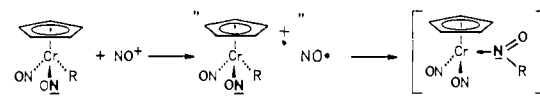

(9)

NO^+ cation could oxidize the $CpCr(NO)_2R$ reagent to its 17-electron radical cation while being itself reduced to NO•. The organometallic cation thus formed could then insert a bound NO into its Cr–R bond, presumably via intramolecular nucleophilic attack of R onto the nitrogen atom of a nitrosyl ligand (underlined in eq 9).[32] Finally, the resulting 15-electron $[CpCr(NO)\{N(O)R\}]^{\bullet+}$ species would be trapped by the still present NO• radical to afford the final dinitrosyl cation shown in eq 9. Note that if this mechanism is indeed operative, then it would be a nitrosyl ligand originally in the chromium's coordination sphere (as opposed to the external NO^+) that would finally constitute a part of the bound RNO group.

(27) Greenhough, T. J.; Kolthammer, B. W. S.; Legzdins, P.; Trotter, J. *Acta Crystallogr., Sect. B* **1980**, *B36*, 795.

(28) Levine, I. N. *J. Chem. Phys.* **1963**, *38*, 2326.

(29) A similar feature has been observed for $[Cp_3Mn_3(\mu_2\text{-}NO)_3(\mu_3\text{-}NOH)]^+PF_6^-$. See: Legzdins, P.; Nurse, C. R.; Rettig, S. J. *J. Am. Chem. Soc.* **1983**, *105*, 3727.

(30) Boyd, A. S. F.; Browne, G.; Gowenlock, B. G.; McKenna, P. *J. Organomet. Chem.* **1988**, *345*, 217 and references therein.

(31) Caulton, K. G. *Coord. Chem. Rev.* **1975**, *14*, 317.

(32) Related oxidatively promoted alkyl to acyl migratory insertions involving $CpFe(CO)(L)Me$ complexes, which are isoelectronic with $CpCr(NO)_2Me$, have been documented. See: Magnuson, R. H.; Meirowitz, R.; Zulu, S.; Giering, W. P. *J. Am. Chem. Soc.* **1982**, *104*, 5790 and references therein.

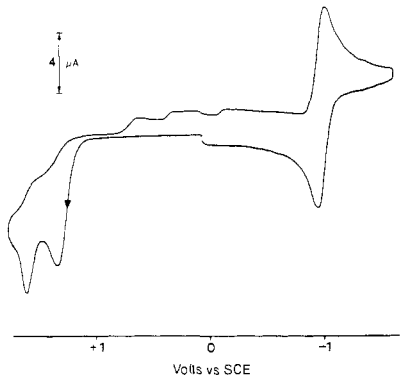

Figure 3. Ambient temperature cyclic voltammogram of 5×10^{-4} M $CpCr(NO)_2Me$ in CH_2Cl containing 0.1 M $[n\text{-}Bu_4N]PF_6$ measured at a platinum-bead electrode at a scan rate of 0.30 V s^{-1}.

Table XV. Cyclic Voltammetry Data for the Oxidations of Some $CpCr(NO)_2R$ Complexes

compd[a]	$E_{p,a}$[b]	scan rate, V s^{-1}
$CpCr(NO)_2Me$	+1.33, +1.55	0.30
$CpCr(NO)_2CH_2SiMe_2$	+1.42	0.39
$CpCr(NO)_2Ph$	+1.32	0.19

[a] In CH_2Cl_2/0.1 M $[n\text{-}Bu_4N]PF_6$. [b] Volts vs SCE, for which the Cp_2Fe–Cp_2Fe^+ couple occurs at +0.46 V ($i_{p,a}/i_{p,c}$ = 1, ΔE = 70 mV).

Any discussion concerning the viability of this mechanism must first involve a consideration of the relative ease of oxidation of the various $CpCr(NO)_2R$ complexes. Consequently, we have investigated the oxidation behavior of these compounds in CH_2Cl_2 by employing cyclic voltammetry at a platinum-bead electrode with $[n\text{-}Bu_4N]PF_6$ as the support electrolyte. A typical cyclic voltammogram, that of $CpCr(NO)_2Me$,[33] is shown in Figure 3, and data for the oxidations of all three compounds are collected in Table XV. The pertinent feature that is immediately evident is that the $CpCr(NO)_2R$ complexes all undergo irreversible oxidations at fairly high potentials (>1.3 V vs SCE). (For comparison, isoelectronic $CpFe(CO)_2Me$ undergoes a similar irreversible oxidation at +1.10 V under identical experimental conditions.) Since the reduction potential of NO^+ in CH_2Cl_2 has been estimated as being in the range −0.22 to −0.11 V,[34] it is unlikely that NO^+ would be able to oxidize the $CpCr(NO)_2R$ species cleanly and completely. To do just that, we chose instead the more potent 1-electron oxidant $[Fe(phen)_3]^{3+}$ whose standard reduction potential is 1.13 V at 25 °C.[35] Indeed, at room temperature in CH_2Cl_2, $CpCr(NO)_2Me$ (ν_{NO} 1777 (s), 1669 (vs) cm^{-1}) is completely converted by 1 equiv of $[Fe(phen)_3]^{3+}$ into a $CpCr(NO)_2^+$-containing product (ν_{NO} 1846 (s), 1745 (vs) cm^{-1}). However, when this oxidation product is treated with NO gas, none of the formaldoxime complex is produced. This state of affairs persists even if the sequential transformations are effected at −78 °C, i.e.

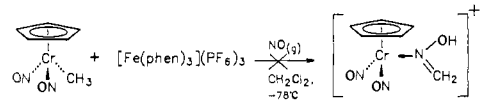

(10)

Furthermore, there is no spectroscopic evidence for the formation of the NO-inserted products when $CpCr(NO)_2CH_2SiMe_3$ and $CpCr(NO)_2Ph$ are treated in the manner depicted in eq 10. While the exact natures of the organometallic products formed in these latter conversions remain to be ascertained, the evidence presently at hand thus argues against reactions 4 proceeding via the mechanistic steps outlined in eq 9.

Scheme I

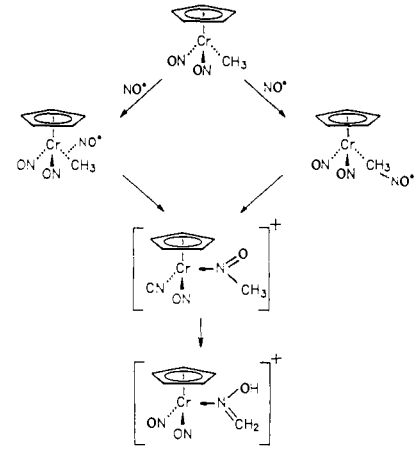

(b) Direct Electrophilic Attack at the Chromium–Carbon Bonds. The second plausible mechanistic pathway for the formation of the NO^+-inserted products of reactions 4 involves charge-controlled, intermolecular attacks by NO^+ at the chromium–carbon σ bonds of the $CpCr(NO)_2R$ reactants. Such a pathway is illustrated for $CpCr(NO)_2Me$ in Scheme I in which the attack by NO^+ is portrayed as being a classical S_E2 process.[36] The isomerization of the CH_3NO ligand to bound CH_2=NOH in the last step of Scheme I has already been demonstrated to occur for the perdeuteromethyl analogue (vide supra) and is probably facilitated by the acidic species present in the reaction mixture.[37] Note that if this mechanism is indeed operative, then it is the external NO^+ (as opposed to a nitrosyl ligand in the organometallic reactant) that finally is a constituent part of the formaldoxime ligand. In other words, treatment of the various $CpCr(NO)_2R$ complexes with electrophiles NE^+, which are formally valence isoelectronic with NO^+, should result in the insertion of NE^+ (and not NO^+) into the Cr–C σ bonds if mechanisms analogous to that portrayed in Scheme I hold. Indeed, that is exactly what is observed experimentally.

Thus, when an aryldiazonium cation (valence isoelectronic with the nitrosonium cation) is used in place of NO^+ in reaction 5, the following conversion occurs:

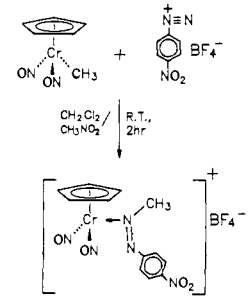

(11)

The final product salt is isolable as a green-brown crystalline solid whose spectroscopic properties are consistent with it possessing the molecular structure shown in eq 11. For instance, a Nujol mull IR spectrum of this moderately air-stable solid displays bands at 1605, 1590, and 1560 cm^{-1} that are assignable to the newly formed diazene ligand. Furthermore, a ^1H NMR spectrum of the complex in CD_3NO_2 exhibits an AX pattern in the δ 8.5–7.2 region due to the protons of a para-substituted phenyl ring and singlets at δ 6.12 and 4.26 due to the cyclopentadienyl and methyl protons, respectively. To confirm the mode of linkage of the *p*-nitrophenylmethyldiazene ligand to the $CpCr(NO)_2$ fragment, the salt was subjected to a single-crystal X-ray crystallographic analysis. The pertinent details of this analysis are collected in

(33) We have analyzed the reduction behavior of $CpCr(NO)_2Me$ in some detail previously. See: Legzdins, P.; Wassink, B. *Organometallics* **1988**, *7*, 482.

(34) Connelly, N. G.; Demidowicz, Z.; Kelly, R. L. *J. Chem. Soc., Dalton Trans.* **1975**, 2335.

(35) Rieger, P. H. *Electrochemistry*; Prentice-Hall: Englewood Cliffs, NJ, 1987; p 455.

(36) Rogers, W. N.; Page, J. A.; Baird, M. C. *Inorg. Chem.* **1981**, *20*, 3521 and references therein.

(37) Boyer, J. H. In *The Chemistry of the Nitro and Nitroso Groups*; Feuer, H., Ed.; Wiley-Interscience: Toronto, 1969; Part 1.

Tables I and II, two views of the solid-state molecular structure of the organometallic cation are shown in Figure 2, and selected intramolecular dimensions of the cation are presented in Table XI. As for the formaldoxime-containing cation (vide supra), the $CpCr(NO)_2$ fragment in the $[CpCr(NO)_2\{N(NC_6H_4NO_2)Me\}]^+$ cation is normal, and the internal dimensions of the diazene ligand are fully in accord with it functioning as a Lewis base toward the chromium center.[38] Interestingly, the diazene ligand adopts a cis configuration, probably for steric reasons, and there is no evidence for the existence of the *trans*-diazene-containing isomer either in the solid state or in solutions. Certainly, the atomic connectivity of the diazene-containing cation in the solid state is consistent with it being formed by the electrophilic attack of external $[p\text{-}O_2NC_6H_4NN]^+$ at the Cr–Me bond of $CpCr(NO)_2Me$.

Similar treatment of $CpCr(NO)_2Me$ in CH_2Cl_2–CH_3NO_2 with $NS^+PF_6^-$ generated in situ affords a thermally unstable green powder whose IR spectrum as a Nujol mull is consistent with its being formulated as $[CpCr(NO)_2\{(NSH)CH_2\}]^+PF_6^-$. The successful incorporation of the thionitrosonium and aryldiazonium cations into these Cr–Me links thus suggests that the formal NO^+ insertion into this and related $CpCr(NO)_2R$ compounds (eq 4) also probably proceeds by direct electrophilic attack as depicted in Scheme I for R = Me.

Stoichiometric Cycle for the Formation of New Carbon–Nitrogen Bonds. As pointed out in the preceding sections, the newly formed nitrosoalkane and diazene ligands in the cationic products of transformations 4 and 11 may be simply viewed as Lewis bases coordinated to the cationic metal center. Consequently, they should, in principle, be displaceable from the chromium's coordination sphere by other, more strongly coordinating 2-electron donors. For practical reasons, we have found that the chloride anion is the Lewis base of choice for effecting these displacement reactions. For example, treatment of a red dichloromethane solution of $[CpCr(NO)_2\{N(O)Ph\}]^+$ at 20 °C with 1 equiv of $[PPN]^+Cl^-$ results in reaction 12,

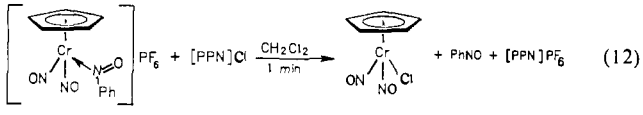

(12)

the nitrosobenzene being isolable from the final reaction mixture by sublimation after removal of the CH_2Cl_2 solvent in vacuo. The success of reaction 12 thus permits the construction of a cycle of stoichiometric reactions for the formation of new carbon–nitrogen bonds mediated by the $CpCr(NO)_2$ group. Such a cycle is shown below for the particular case of NO^+ insertion, Cr representing the metal center in the $CpCr(NO)_2$ group:

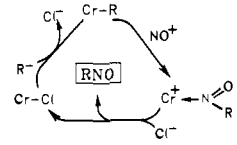

Thus, when R = Ph, reaction 12 is shown at the bottom of the cycle. The $CpCr(NO)_2Cl$ byproduct of this reaction may be reconverted to the original $CpCr(NO)_2Ph$ reactant simply by treatment with Ph_3Al,[14] and the insertion of NO^+ may then be effected again. In principle, cycles similar to that shown above should also hold for R = Me or CH_2SiMe_3 and for NS^+ or $[p\text{-}O_2NC_6H_4N_2]^+$ as the electrophile in place of NO^+. Our preliminary investigations indicate that this is indeed true and that it usually is not necessary to isolate the intermediate insertion products. Thus, sequential treatment of $CpCr(NO)_2Ph$ with $[p\text{-}O_2NC_6H_4N_2]^+BF_4^-$ and then $[PPN]^+Cl^-$ affords good yields of the unsymmetrical diazene, $p\text{-}O_2NC_6H_4N{=}NPh$,[39] and $CpCr(NO)_2Cl$.

The net organic transformation mediated by the $CpCr(NO)_2R$ groups in cycles such as that shown above are thus

$$NE^+ + R^- \rightarrow N(E)R \qquad (13)$$

where NE^+ is the external nitrogen-containing electrophile and R^- is the organic group initially σ-bonded to chromium. The final N(E)R product is formed selectively, the new C–N linkage being generated exclusively at the carbon atom originally attached to the metal center. At present, it appears that the $CpCr(NO)_2R$ compounds undergo the requisite insertion of NE^+ into the Cr–R bonds because these bonds are prone to nonoxidative attack by electrophiles and the compounds themselves are relatively difficult to oxidize. In principle, therefore, it should be possible to broaden the scope of this synthetic methodology by extending this chemistry to encompass a wide range of $CpCr(NO)_2$-containing organometallic complexes and other electrophiles.

Acknowledgment. We are grateful to the Natural Sciences and Engineering Research Council of Canada for support of this work in the form of grants to P.L. and F.W.B.E. and a postgraduate scholarship to B.W. We also thank The University of British Columbia for the award of a graduate fellowship to G.B.R.-A.

Supplementary Material Available: Tabulations of the atomic coordinates of the hydrogen atoms, the anisotropic thermal parameters, additional distances and angles, and least-squares planes for $[CpCr(NO)_2\{N(OH)CH_2\}]^+PF_6^-$ and $[CpCr(NO)_2\{N(NC_6H_4NO_2)Me\}]^+BF_4^-$ (7 pages); listings of observed and calculated structure factors (29 pages). Ordering information is given on any current masthead page.

(38) Einstein, F. W. B.; Sutton, D.; Tyers, K. G. *Inorg. Chem.* **1987**, *26*, 111 and references therein.

(39) Christoforou, D.; Happer, D. A. R. *Aust. J. Chem.* **1983**, *36*, 2083.